MOLECULAR AND CELLULAR BIOLOGY, Mar. 1984, p. 454–467
0270-7306/84/030454-14$02.00/0

Vol. 4, No. 3

Size-Variant pp60^{src} Proteins of Recovered Avian Sarcoma Viruses Interact with Adhesion Plaques as Peripheral Membrane Proteins: Effects on Cell Transformation

JAMES G. KRUEGER, ELLEN A. GARBER, STEVEN S.-M. CHIN, HIDESABURO HANAFUSA, AND ALLAN R. GOLDBERG*

The Rockefeller University, New York, New York, 10021

Received 18 August 1983/Accepted 9 December 1983

We have shown previously that the membrane association of the *src* proteins of recovered avian sarcoma viruses (rASVs) 1702 (56 kilodaltons) and 157 (62.5 kilodaltons), whose size variations occur within 8 kilodaltons of the amino terminus, is salt sensitive and that, in isotonic salt, these *src* proteins fractionate as soluble cytoplasmic proteins. In contrast, wild-type Rous sarcoma virus pp60^{src} behaves as an integral plasma membrane protein in cellular fractionation studies and shows prominent membrane interaction by immunofluorescence microscopy. In this study we have examined the distribution of these size-variant *src* proteins between free and complexed forms, their subcellular localization by immunofluorescence microscopy, and their ability to effect several transformation-related cell properties. Glycerol gradient sedimentation of extracts from cells infected either with rASV 1702 or rASV 157 showed that soluble *src* proteins of these viruses were distributed between free and complexed forms as has been demonstrated for wild-type Rous sarcoma virus pp60^{src}. Pulse-chase studies with rASV pp60^{src} showed that, like wild-type Rous sarcoma virus pp60^{src}, it was transiently found in a complexed form. Indirect immunofluorescence showed that size-variant pp60^{src} proteins are localized in adhesion plaques and regions of cell-to-cell contact in rASV 1702- or 157- infected cells. This result is in contrast with the generalized localization of pp60^{src} in plasma membranes of control rASV-infected cells which produce pp60^{src}. Chicken embryo fibroblasts infected by rASVs 1702 and 157 display a partial-transformation phenotype with respect to (i) transformation-related morphology, (ii) cell surface membrane changes, and (iii) retained extracellular fibronectin. It is possible that the induction of a partial-transformation phenotype may be the result of the unique interaction of the *src* proteins encoded by these viruses with restricted areas of the plasma membrane.

Cellular transformation by Rous sarcoma virus (RSV) is mediated by the *src* gene product pp60^{src}, a 60,000-dalton phosphoprotein possessing tyrosine-specific kinase activity (7, 25). Recent studies in which immunofluorescence microscopy, electron microscopic immunocytochemistry, and subcellular fractionation were used (8, 9, 20–22, 24, 27, 31, 33, 36, 37, 42) have indicated that pp60^{src} in RSV-transformed chicken embryo fibroblasts (CEF) is predominantly associated with the cytoplasmic face of the plasma membrane and specialized portions of the plasma membrane such as adhesion plaques and regions of cell-cell contact. pp60^{src} appears to behave as an integral membrane protein (11, 20, 21, 24). The interaction of pp60^{src} with membranes is mediated by an amino-terminal domain (20, 21, 24) whose hydrophobicity is due, at least in part, to tightly bound lipid (11, 34). pp60^{src} is synthesized on free polyribosomes (23, 29), becoming membrane associated shortly after synthesis (26). Characterization of the interaction of pp60^{src} with two cellular phosphoproteins, pp50 and pp90, suggests that the pp50-pp60^{src}-pp90 complex may be the vehicle by which pp60^{src} is transported through the cytoplasm to the plasma membrane (4, 8).

Two isolates of recovered avian sarcoma viruses (rASVs), 1702 and 157, encode pp60^{src} proteins with alterations in the amino-terminal membrane binding domain (17). rASVs 1702 and 157 *src* proteins show altered membrane association, displaying a salt-sensitive subcellular distribution and fractionating as soluble, cytoplasmic proteins in isotonic salt (19). Although the amino-terminal alterations do not interfere with kinase activity or the ability to effect a number of transformation parameters of infected CEF cells in culture, the in vivo tumorigenicity of these viruses is greatly reduced (19) and their *src* proteins contain no detectable lipid (11). One other soluble *src* protein has been described: in tsNY68-infected cells maintained at the nonpermissive temperature (41 to 42°C), pp60^{src} is a soluble cytoplasmic protein found almost exclusively in the pp50-pp90 complexed form (4, 8, 12). At the nonpermissive temperature, both the in vivo tumorigenicity of tsNY68 (18, 28) and the amount of lipid associated with pp60^{src} (11) are reduced. However, in contrast to rASV 1702- or 157-infected cells, which appear morphologically transformed, tsNY68-infected cells at the nonpermissive temperature do not appear morphologically transformed and show reduced kinase activity (7, 18, 25). To elucidate further the nature of the interaction of soluble *src* proteins with subcellular components in rASV 157- and rASV 1702-infected cells and to clarify the similarities and differences between these amino-terminally altered pp60^{src} proteins and tsNY68 pp60^{src}, we have examined (i) the interaction of these *src* proteins with the pp50-pp90 complex, (ii) the intracellular localization of these pp60^{src} proteins, (iii) the morphology of cells transformed by these viruses by scanning electron microscopy, (iv) the organization of cytoskeleton, adhesion plaques, and fibronectin in rASV-transformed cells by immunofluorescence microscopy, and (v) the biochemical properties of the rASV 1702 *src* protein. These data suggest that rASV 1702 and rASV 157 *src* proteins behave as peripheral membrane proteins in contrast to wild-type pp60^{src} which behaves as an integral membrane protein or to tsNY68 pp60^{src} (at a restrictive temperature) which behaves as a soluble cytosolic protein. Observations on cells transformed by rASVs whose *src*

* Corresponding author.

proteins have amino-terminal alterations suggest that adhesion plaque localization and generalized plasma membrane localization of pp60^{src} may be separable phenomena.

MATERIALS AND METHODS

Cells and viruses. CEF were grown in monolayer culture and infected with the Schmidt-Ruppin strain of RSV subgroup A, its temperature-sensitive mutant tsNY68, or td 109-derived rASV isolates 157, 1702, or 3811 as previously described (12, 17, 19, 20).

Antisera. Tumor-bearing rabbit (TBR) serum was obtained as previously described (7). pp60^{src}-specific antiserum was prepared from TBR serum by adsorption to an Affigel matrix to which viral structural proteins had been covalently linked (20); this antiserum has been used previously to localize pp60^{src} in CEF transformed by RSV and tsNY68 (12). Filamin was prepared from a chicken gizzard by the method of Shizuta et al. (35) and purified to homogeneity as judged by sodium dodecyl sulfate (SDS)-polyacrylamide gel electrophoresis analysis. Anti-filamin antibodies were raised in a rabbit which was initially injected intramuscularly with 6 mg of purified filamin mixed with Freund adjuvant and subsequently boosted intravenously over a period of 5 months with a total of 5 mg of filamin dissolved in aqueous buffer. The resulting antisera contained antibodies specifically directed against filamin as determined by immunodiffusion and immunoprecipitation reactions. Goat antisera to chicken fibronectin was obtained from Calbiochem-Behring, La Jolla, Calif.

Immunoprecipitation of radiolabeled proteins and protein kinase assay. Cells were labeled with [^{3}H]leucine at 1 mCi/ml for the specified period of time in leucine-free Dulbecco modified essential medium containing 5% dialyzed calf serum. For pulse-chase studies, transformed cells were starved of leucine for 60 min, labeled with [^{3}H]leucine for 20 min, and either harvested or washed and incubated with Dulbecco modified essential medium containing 5% calf serum and 10 times the normal concentration of leucine. Cell extracts were immunoprecipitated with TBR serum, and immunoprecipitated proteins were analyzed by electrophoresis on 10% SDS-polyacrylamide gels as previously described (12). Kinase activity in immune complexes was assayed as described previously (21). Radioactivity in gel bands was quantitated as previously described (11).

Glycerol gradient sedimentation. Cells were washed three times with phosphate-buffered saline (PBS) and lysed at 4°C in modified RIPA buffer (10 mM Tris-hydrochloride [pH 7.2], 150 mM NaCl, 1 mM EDTA, 1 mM EGTA [ethylene glycol-bis(β-aminoethyl ether)-*N,N*-tetraacetic acid], 1% Triton X-100, 1% sodium deoxycholate, 0.1% SDS). Lysates were clarified by centrifugation at 15,000 × *g* for 10 min. Extracts were layered on 10 to 30% glycerol gradients in modified RIPA buffer and sedimented for 17 h at 49,000 rpm at 4°C in an SW50.1 rotor as described by Brugge et al. (3). Fractions were collected and immunoprecipitated with TBR serum. Immunoprecipitated proteins were analyzed by electrophoresis on 10% SDS-polyacrylamide gels. Autoradiograms of such analyses represent sedimentation (in the glycerol gradient) from right to left.

Immunofluorescence microscopy. Cells that had been grown in monolayer culture on glass cover slips were washed with PBS and fixed at room temperature for 20 min in PBS containing 3.5% (wt/vol) paraformaldehyde. The fixed cells were rinsed with PBS and permeabilized by a 5-min treatment with 1% Triton X-100 in PBS. Cover slips were washed twice with 1% glycine (wt/vol) in PBS and then incubated with pp60^{src}-specific serum or rabbit antiserum raised against purified filamin for 1 h at 37°C in a humid chamber. Cover slips were washed three times with PBS at 37°C and then incubated for 30 min at 37°C in a humid chamber with fluorescein-conjugated goat anti-rabbit immunoglobulin G that had been preadsorbed against CEF cells. Cover slips again were washed with PBS at 37°C and mounted for microscopic analysis. For visualization of the F-actin-containing cytoskeleton, fixed, permeabilized cells were stained with 7-nitrobenz-2-oxa-1,3-diazole (NBD)–phallacidin (132 ng/ml) in PBS for 30 to 60 min in a humid chamber at 37°C (2). To visualize extracellular fibronectin, a 1:20 dilution of anti-fibronectin serum was incubated with fixed but unpermeabilized cells for 30 min at 37°C. After these cells were washed with PBS, they were incubated with a 1:20 dilution of fluorescein-conjugated rabbit anti-goat immunoglobulin G for an additional 30 min at 37°C. Cover slips were washed with warm PBS and mounted. Mounted cover slips were viewed through X63 oil-immersion objectives with a Zeiss photomicroscope equipped with epifluorescent illumination. All photomicrographs in this manuscript have a magnification of X316 at the camera photographic plate but were enlarged during photographic printing to display different cellular details. Photographs were taken on Kodak Tri-X film at ASA 1,600.

Scanning electron microscopy. Cells grown on glass cover slips were fixed in half-strength Karnofsky fixative (2.5% glutaraldehyde, 2% formaldehyde, 0.1 M sodium phosphate [pH 7.4], saturated $CaCl_2$) and postfixed with 2% OsO_4 in 0.1 M sodium phosphate (pH 7.4). Fixed cells were dehydrated through graded alcohols into acetone and were critical-point dried in liquid CO_2. After the cells were coated with Au-Pd, they were viewed with an accelerating voltage of 25 kV in a JEOL JSM 35 scanning electron microscope, and micrographs were recorded on Polaroid type-55 film.

Preparation of cytoskeleton matrices. Cytoskeleton matrices were prepared by extracting transformed cells with CSK buffer, using standard procedures (5, 6). CSK buffer contains 10 mM PIPES [piperazine-*N,N'*-bis (2-ethanesulfonic acid); pH 6.8], 1% Nonidet P-40 (NP-40), 300 mM sucrose, and either 2.5 mM $MgCl_2$ or 2.5 mM EDTA. KCl was added to this buffer in concentrations from 10 to 500 mM in individual experiments. To prepare cytoskeleton matrices, 60-mm plates of rASV 1702- or RSV-transformed cells were washed three times with PBS and two times with CSK buffer without NP-40. CSK buffer containing 1% NP-40 was then added to each plate and allowed to incubate for 2 min on ice, after which the supernatant was collected. The residual cytoskeleton matrix remaining on the dish was washed two times with CSK buffer containing NP-40 and then removed from the dish by scraping into CSK buffer containing 1% sodium deoxycholate, 0.1% SDS, and 1% NP-40. After adding sodium deoxycholate and SDS to the supernatant fraction to the same concentration as that in the cytoskeleton matrix fraction, fractions were clarified by centrifugation at 15,000 × *g* for 10 min, and pp60^{src} kinase activity was measured as previously described (21). The amount of pp60^{src} solubilized by this procedure is expressed as a percentage of total kinase contained in detergent-soluble (supernatant) and detergent-insoluble (cytoskeleton) fractions. Recovery of total cellular kinase was 100% of that obtained by direct lysis of whole cells under standard kinase assay conditions.

RESULTS

Analysis of pp60^{src} in free and complexed forms. The interaction of rASV-encoded *src* proteins with the pp50-pp90

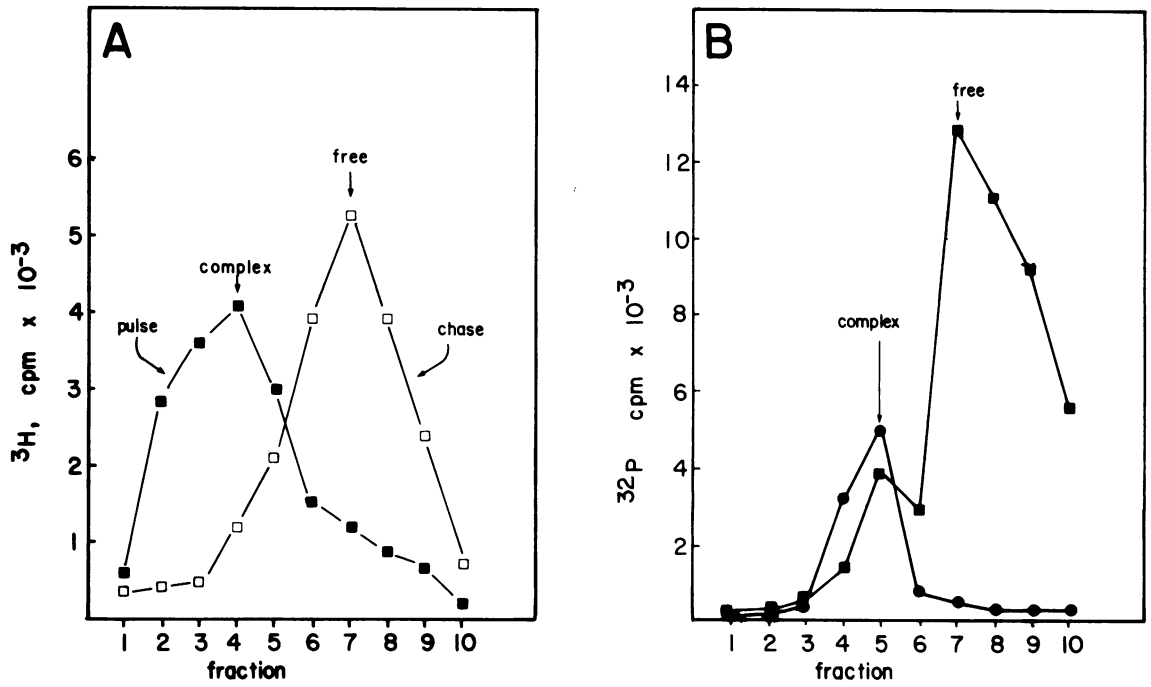

FIG. 1. Glycerol gradient sedimentation analysis of pp60^{src} from rASV 1702-transformed CEF. (A) Quantitation of [^{3}H]leucine pulse-chase. rASV 1702-transformed cells were labeled for 20 min with [^{3}H]leucine, and cell lysates were analyzed by glycerol gradient sedimentation immediately after the pulse (■) or after a 3-h chase (□). The 56-kilodalton *src* polypeptide was excised from SDS-polyacrylamide gels, and radioactivity in gel slices was quantitated. (B) Glycerol gradient sedimentation profile of pp60^{src} kinase activity from CEF infected by tsNY68 maintained at 42°C (●) or from cells transformed by rASV 1702 (■). The peak positions of monomeric, free pp60^{src} (fraction 7) and the complex (fraction 5) were determined from parallel analysis of lysates from labeled cells. Fraction 1 is at the bottom of each gradient.

complex was examined by glycerol gradient centrifugation of lysates of CEF transformed by rASV 3811, which encodes a 60-kilodalton *src* protein that behaves as an integral membrane protein, and by rASV 1702 or rASV 157, which encode size-variant *src* proteins that behave predominantly as soluble cytoplasmic proteins in cell fractionation studies (19). Immunoprecipitation with TBR serum of gradient fractions from lysates of cells labeled for 4 h with ^{32}P showed the distribution of rASV 3811, rASV 1702, rASV 157 pp60^{src} proteins between free and complexed forms (data not shown) was like that described for wild-type SR-RSV pp60^{src}: only a small fraction was found complexed, whereas the vast majority of pp60^{src} was found in the free form (3, 4). As determined by *Staphylococcus aureus* V8 protease mapping of the pp60^{src} immunoprecipitated from each fraction (data not shown), rASVs 3811, 1702, and 157 *src* proteins in the complex are underphosphorylated on tyrosine 416 compared with free pp60^{src} and in this respect are also similar to wild-type pp60^{src} (3, 4, 8).

These results suggested that the size-variant *src* proteins encoded by rASVs 1702 and 157 interact with the complex-like wild-type pp60^{src}. To test whether the kinetics of the interaction of rASV 1702 pp60^{src} with the complex are similar to those of wild-type pp60^{src}, we carried out the pulse-chase experiment whose results are quantitated in Fig. 1A. rASV 1702-transformed cells were pulse-labeled for 20 min with [^{3}H]leucine and either harvested immediately or chased for 3 h in medium containing excess unlabeled leucine, and cell lysates were analyzed by glycerol gradient sedimentation, immunoprecipitation, and SDS-polyacryl-

FIG. 2. Localization of pp60^{src} in CEF transformed by the Schmidt-Ruppin strain of RSV, subgroup A. The focal plane was set at approximately mid-nuclear level (A) or at the ventral cell surface (B and C). pp60^{src} is located in plasma membranes (m), at regions of cell-to-cell contact (c), and in adhesion plaques (ap).

amide gel electrophoresis. The 56-kilodalton rASV 1702 *src* protein bands were excised from gels, and the radioactivity in each band was quantitated. Newly synthesized pp60^{src} was found principally in the complex (fractions 2 through 5). After a 3-h chase, rASV 1702 pp60^{src} was no longer found complexed but was found primarily in monomeric form in fractions 6 through 8. These data suggest that rASV 1702 *src* protein, like wild-type pp60^{src}, transiently exists in a complexed form shortly after its biosynthesis.

Previous attempts to demonstrate kinase activity of pp60^{src} in the complex have been unsuccessful (3, 8), possibly because RIPA buffer was used throughout these experiments. For determination of kinase activity in the experiments described below, glycerol gradient fractions were immunoprecipitated in RIPA buffer, but immune complexes were washed in a less denaturing Triton X-100-containing buffer which allows greater recovery of kinase activity than does RIPA buffer (21). pp60^{src} in the complex from both tsNY68- and rASV 1702-transformed cells has demonstrable kinase activity (Fig. 1B) which parallels the distribution of labeled pp60^{src} observed in parallel gradients (data not shown): tsNY68 (at 42°C) kinase activity is associated with complexed pp60^{src}, whereas rASV 1702 kinase activity is distributed between free and bound forms. In rASV 1702, kinase specific activity is essentially equal in both the free and bound forms. The kinase specific activity in the complexed form of tsNY68 pp60^{src} at 42°C is reduced by about the same amount (ca. fourfold) as the whole cell kinase specific activity is reduced (data not shown).

Localization of pp60^{src} by immunofluorescence microscopy. Size-variant pp60^{src} proteins encoded by rASVs 1702 and 157 appear to interact only transiently with the pp50-pp90 complex and might therefore be transported to specific subcellular sites. To examine this possibility, immunofluorescence microscopy was used to localize pp60^{src} in cells transformed by soluble pp60^{src} proteins as well as cells transformed by control, membrane-bound pp60^{src} proteins. The staining of pp60^{src} in RSV-transformed CEF by pp60^{src}-specific antiserum is shown in Fig. 2. pp60^{src} is seen in the free cell edge and in cell-to-cell contact regions when the focal plane is set at approximately midnuclear or midcytoplasmic level (Fig. 2A). This membrane-staining pattern is not evident when the focal plane is set at the level of the ventral plasma membrane or substratum, at which cells attach to the glass cover slips (Fig. 2B). In some RSV-transformed CEF (a subpopulation of cells which are well spread on the glass surface), pp60^{src} also can be observed in discrete fluorescent spots near the ventral cell surface (Fig. 2C). When cells with this pattern of fluorescence are examined by interference reflection microscopy (data not shown), these fluorescent pp60^{src}-containing spots coincide with adhesion plaques, confirming the previous results of Rohrschneider (32). In the following discussion, the term adhesion plaque refers to punctate areas of cell-substratum adhesion which are seen as dark spots or streaks by interference reflection microscopy. A more detailed description of the types of cell-substratum adhesions occurring in normal CEF and in CEF transformed by RSV and rASVs is presented in a separate section below. It is not possible to detect pp60^{src} in adhesion plaques of RSV-transformed cells that are extremely round and poorly spread such as those shown in Fig. 2B. As a control for these experiments, we detected no pattern of specific staining when this TBR serum was reacted with untransformed CEF (Fig. 3A) or when serum from normal rabbits was reacted with any of the cell types described in this study. In CEF transformed by rASV 1702, pp60^{src} was present in abundant adhesion plaques which occurred in clusters beneath the nucleus and at the edge of the cell (Fig. 3B). The localization of pp60^{src} in adhesion plaques of all rASV-transformed cells was confirmed by interference reflection microscopy but is shown only in selected examples. In subconfluent cultures, cells appeared to form intercellular contacts through cytoplasmic extensions or projections. At points of contact, pp60^{src} often can be seen in single or small groups of adhesion plaque-like structures which form at the level of the substratum in both cells (Fig. 3B, arrow). The correspondence of pp60^{src} staining with adhesion plaques is clearly seen in rASV 1702-transformed cells examined by immunofluorescence and interference reflection microscopy (Fig. 3C and D). The adhesion plaques occurring in these cells are abnormally large clumps and clusters which differ from adhesion plaques in both uninfected and RSV-transformed CEF (see below). In many rASV 1702-transformed cells, pp60^{src} can be seen both in adhesion plaques and in plasma membranes at regions of cell-to-cell contact. Figures 3E and F show a cell pair which was photographed at different focal levels: pp60^{src} is seen clearly in adhesion plaques located near the ventral cell surface (Fig. 3F) and in cell-to-cell contacts at a higher focal plane (Fig. 3E). Note that many of the pp60^{src}-containing adhesion plaques form in clusters at the boundary region between the two cells and underneath the region of cell-to-cell contact. In rASV 1702-transformed CEF, pp60^{src} was not observed at the free cell edge as it was in RSV-transformed CEF (cf. Fig. 2A and 3E).

rASV 157-transformed CEF, which contain a soluble *src* protein (like rASV 1702-transformed CEF), also show pp60^{src} localized in adhesion plaques and at regions of cell-to-cell contact. Figure 3G shows rASV 157 pp60^{src} in adhesion plaques which occur in large peripheral clusters and a subnuclear rosette. In a large series of experiments, we have observed a remarkably similar, if not identical, pattern of pp60^{src} localization in rASV 1702- and rASV 157-transformed cells. pp60^{src} was seen in abundant adhesion plaques and at focal regions of cell-to-cell contact in sparse and dense cultures of both cell types. Neither cell type showed conspicuous interaction of pp60^{src} with the free cell edge or membrane, though occasional fluorescence was observed in ruffling cell edge membranes (data not shown). This pattern contrasts strikingly with the fluorescence pattern of pp60^{src} in CEF transformed by rASV 3811, which encodes a normal-sized pp60^{src} that is strongly bound to cellular membranes. In Fig. 3H, pp60^{src} is clearly seen in the free cell edge in many of these cells, indicating a generalized interaction with the plasma membrane. Some areas of cell-to-cell contact appear to show increased fluorescent intensity, suggesting that pp60^{src} also is localized in opposing plasma membranes at regions of intercellular contact or in membrane junctions. A generalized interaction of pp60^{src} with plasma membranes also is seen by immunofluorescence microscopy in CEF transformed by rASVs 374 and 1441, both encoding normal-sized pp60^{src} proteins which appear to be integrated into plasma membranes (data not shown).

Analysis of transformed CEF by scanning electron microscopy. CEF tranformed by RSV and rASVs 1702 and 157 were viewed by scanning electron microscopy to examine transformation-related changes in cell morphology and surface topology. Normal CEF are extremely flat cells with a regular, smooth dorsal cell surface. Surface projections such as microvilli or membrane blebs are not seen in normal cells (Fig. 4A). RSV-transformed CEF are quite round when fully transformed and display uniform cell surface changes, including extensive microvillus projections in some cells (Fig.

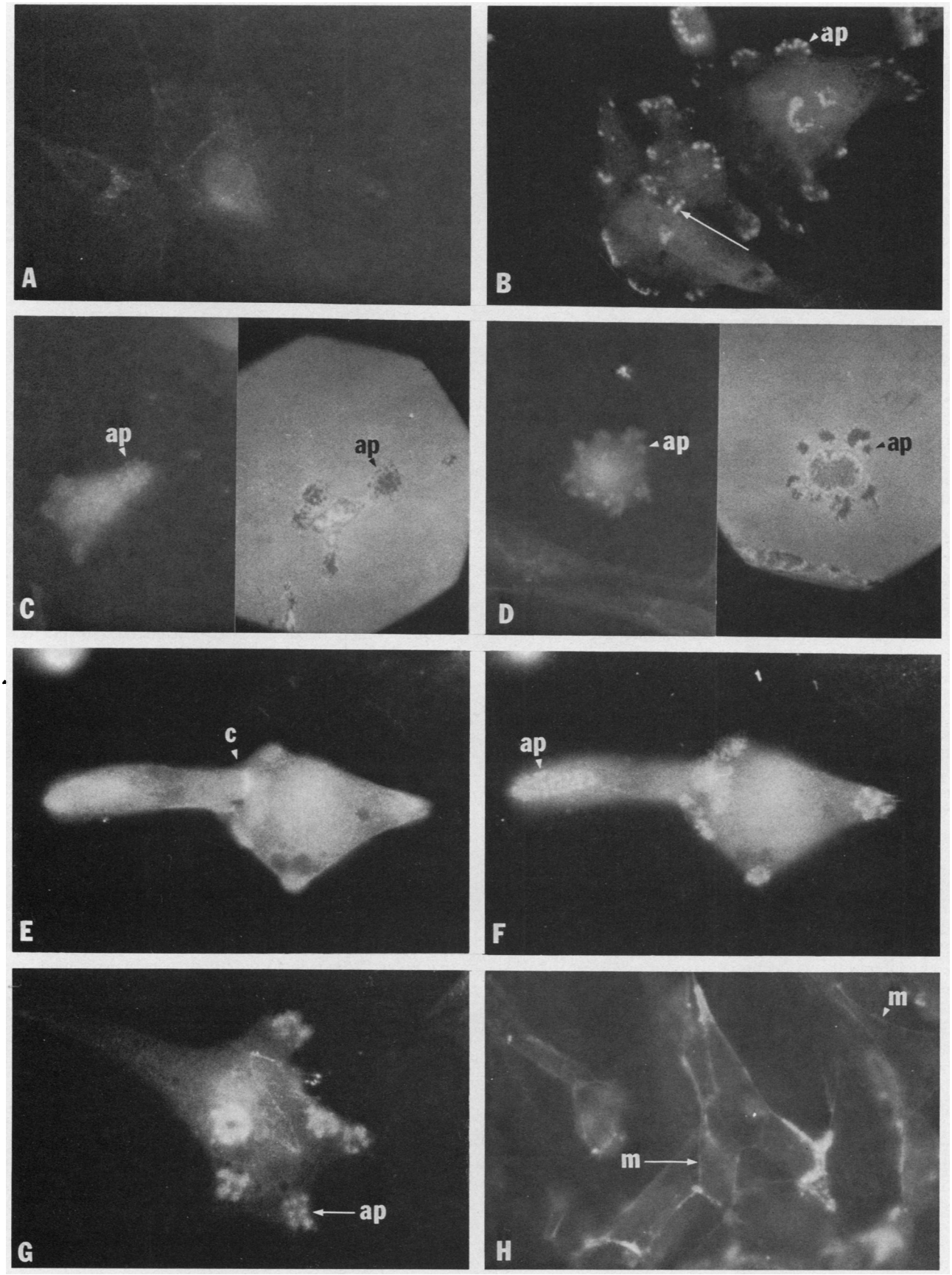
A
B
ap
C
ap
ap
D
ap
ap
E
c
F
ap
G
ap
H
m
m

4B). The surface topology of RSV-transformed CEF (Fig. 4B) is similar to that shown previously for CEF transformed by tsNY68 (40) and is typical of a round, transformed morphology. The shape of rASV 1702- and 157-transformed cells varies from a spindle form to quite flat morphologies (Fig. 4C through F). CEF transformed by rASVs encoding size-variant pp60^{src} proteins display large cell surface blebs and small microvilli which tend to occur in clusters on the dorsal cell surface (Fig. 4C through F). Dorsal surface blebs are an important characteristic of CEF transformed by the RSV partial transformation mutant CU2 (1), which also has large, abundant adhesion plaques containing pp60^{src}. The appearance of dorsal surface blebs in CEF transformed by CU2 and rASVs 1702 and 157 could be related to the presence of abundant pp60^{src}-containing adhesion plaques or to the interaction of pp60^{src} with focal membrane regions. It is interesting to note that dorsal surface blebs and microvilli in rASV 1702- and 157-transformed cells appear to roughly parallel the localization of pp60^{src} in underlying adhesion plaques. However, the precise relationship between these two features cannot be ascertained because of inherent differences in microscopic techniques.

Adhesion plaque structure and organization in rASV-transformed cells. CEF infected with the RSV partial transformation mutant CU2 show a flat, well-spread morphology with small dorsal surface blebs and overproduce adhesion plaques containing pp60^{src} (1, 30, 33). The flatter morphology of cells transformed by rASVs 1702 and 157 and the presence of dorsal surface blebs on both cell types suggested that they might contain an increased abundance of adhesion plaques as do CU2-transformed CEF. Since adhesion plaques have previously been shown to contain actin and filamin (30), in addition to other cytoskeleton proteins, we used NBD-phallacidin (which reacts specifically with F-actin [2]) and anti-filamin antibodies to study the abundance and organization of adhesion plaques in cells transformed by RSV and different rASVs.

Figure 5 displays paired micrographs of NBD-phallacidin fluorescence and interference reflection patterns in uninfected CEF and in cells transformed by RSV and rASVs 3811, 1702, and 157. As defined by Izzard and Lochner (15), cell-substratum adhesions in normal chick fibroblasts consist of focal adhesions and close contacts. Focal adhesions are small, streaklike areas of close (10- to 15-nm) cell-substratum contact and appear black in interference micrographs (Fig. 5A, arrowheads). Close contacts are larger, patchlike areas in which the ventral cell surface is separated by ca. 30 nm from the substrate and appear grey in interference micrographs (Fig. 5A, arrow). White areas in interference micrographs are regions in which the ventral cell surface is separated by 100 to 150 nm from the substratum. In Fig. 5A, note that actin stress fibers seen by NBD-phallacidin staining clearly terminate in streaklike focal adhesions (which are also called adhesion plaques). RSV-transformed CEF are characterized by fewer focal adhesions and close contacts than are in normal cells (Fig. 5B). Remaining focal adhesions tend to be arranged at the cell periphery and appear to be different from smaller, F-actin-containing punctate adhesions which are distributed randomly in the ventral cell surface (Fig. 5B, arrowheads). Differences between normal-appearing focal adhesions and smaller punctate adhesions are seen more clearly in the rASV 3811-transformed cell shown in Fig. 5C, in which black-colored streaklike focal adhesions and grey-colored, punctate adhesions are present in the same cell. The grey color of the punctate adhesions implies greater cell-substratum separation than occurring in normal-appearing focal adhesions. Although the interference color of these punctate adhesions is similar to that of close contacts, it is most likely that they are abnormal focal adhesions, because they are extremely small and the residual actin stress fibers which transverse the cell appear to originate and terminate in some of the punctate adhesions (Fig. 5C). An occasional rASV 3811-transformed cell displays numerous short actin cables which are arranged in a cagelike fashion (Fig. 5D). The apparent ability of the punctuate adhesion to serve as stress fiber termini is well illustrated in transformed cells with this type of actin organization (Fig. 5D). CEF transformed by rASV 157 (Fig. 5E) and by rASV 1702 (Fig. 5F) show even more disordered cell-substratum adhesions than do RSV- or rASV 3811-transformed cells. Normal-appearing focal adhesions are largely absent from these cells, whereas cell-substratum adhesions appear to be mediated by large F-actin-containing aggregates which appear grey in interference micrographs (note that one or two black-colored focal adhesions are present in the rASV 1702-transformed cells shown in Fig. 5F). Since residual actin cables emanate from these cell-substratum contact areas in some cells (see below), it is likely that these adhesions are higher ordered aggregates of the punctate adhesions seen in Fig. 5C.

Some additional features of actin organization in rASV-transformed CEF are illustrated in Fig. 6. In CEF transformed by rASV 157 (Fig. 6B) and rASV 1702, adhesion plaque clusters vary in size and may be organized into scrolls and linear arrays in some cells. These actin-containing clusters frequently occur at regions of cell-to-cell contact in CEF transformed by rASV 1702 (Fig. 6C) and rASV 157. Actin stress fibers are greatly decreased in these rASV-transformed cells compared with those in uninfected controls (Fig. 6A). However, residual actin fibers are present in some transformed cells and can usually be seen terminating in abnormal adhesion plaque clusters (Fig. 6C).

The pattern of filamin staining in these cells is similar to that seen with NBD-phallacidin. Filamin is present in stress fibers in uninfected CEF (Fig. 6D), whereas in rASV 157-transformed CEF it is present in adhesion plaque aggregates and in residual stress fibers which terminate in these aggregates (Fig. 6E). Filamin also is present in actin-containing clusters which occur at regions of cell-to-cell contact in CEF transformed by rASVs 1702 and 157 (data not shown). The colocalization of actin, filamin, and pp60^{src} in plasma membranes at regions of cell-to-cell contact suggests the formation of an adhesion junctionlike structure (37) in these cells and is a characteristic feature of CEF transformed by rASVs

FIG. 3. Localization of pp60^{src} in rASV-transformed cells. Antiserum specific for pp60^{src} was reacted with uninfected cells (A) or with cells transformed by rASV 1702 (B through F), rASV 157 (G), or rASV 3811 (H). The arrow (B) indicates pp60^{src} in adhesion plaquelike structures at regions of cell-to-cell contact. Micrographs C and D are paired immunofluorescence-interference reflection images of pp60^{src} fluorescence and adhesion plaques in the same cell. Micrographs E and F show the same cells which have been photographed at mid-cytoplasmic or mid-nuclear level (E) and at the focal plane of the ventral cell surface (F). The localization of pp60^{src} in adhesion plaques (ap), regions of cell-to-cell contact (c), or the plasma membrane (m) is indicated. Focus was set at the ventral cell surface in all micrographs except E and H, in which it was set at approximately mid-nuclear level.

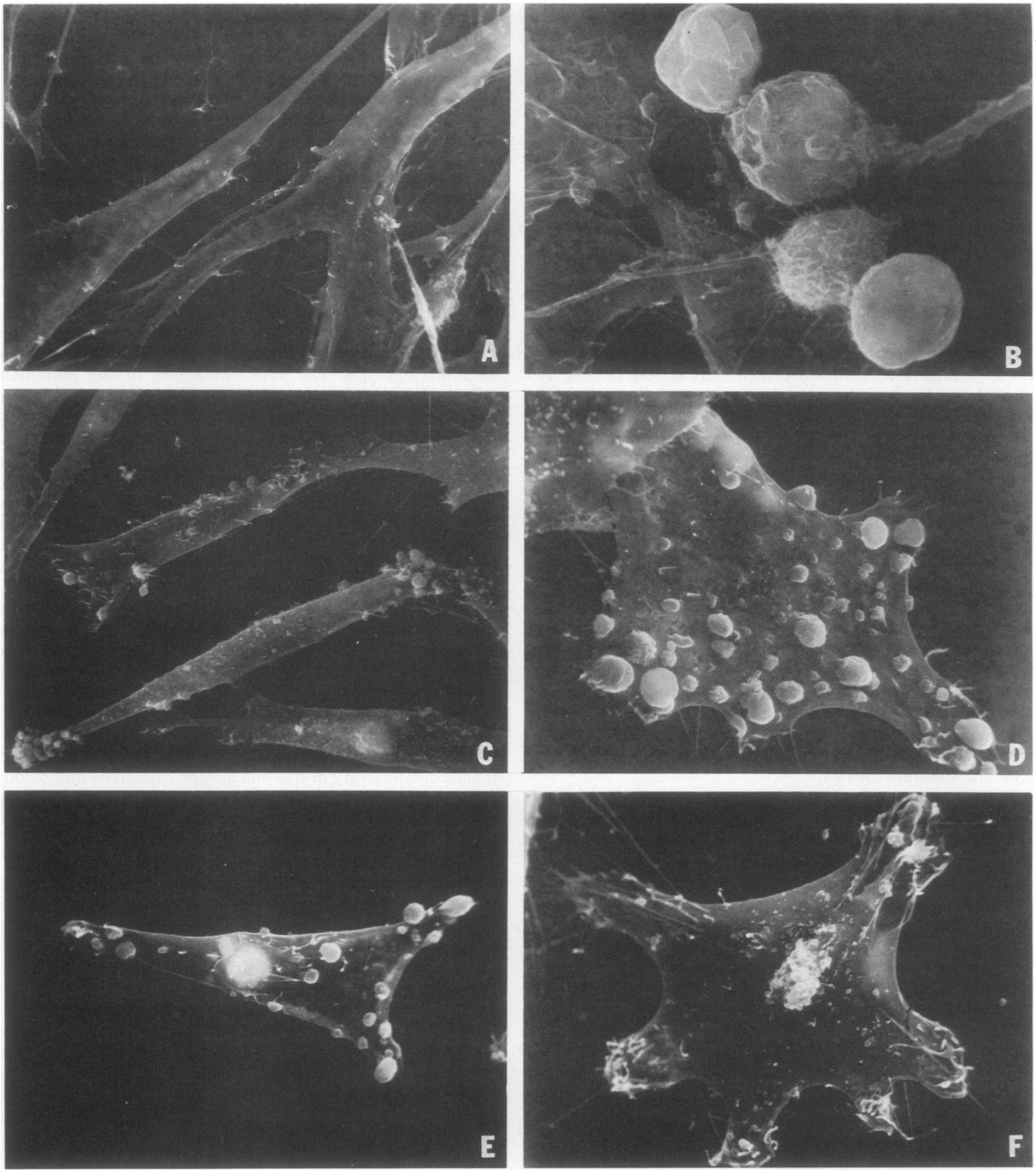

FIG. 4. Analysis of RSV- or rASV-transformed cells by scanning electron microscopy. (A) Normal CEF, ×1,900, (B) RSV-transformed CEF ×2,600, (C) rASV 1702-transformed CEF, ×1,600, (D) rASV 1702-transformed CEF, ×2,600, (E) rASV 157-transformed CEF, ×1,600, (F) rASV 157-transformed CEF, ×2,600.

1702 and 157. In fully rounded cells transformed by rASV 3811 or RSV, filamin is no longer seen in stress fibers but appears to outline the peripheral edge of the cell (Fig. 6F).

Fibronectin staining of rASV-transformed CEF. Rohrschneider and Rosok (30) showed that the presence of $pp60^{src}$ in adhesion plaques correlated with the disappearance of the extracellular fibronectin matrix in CEF infected with a number of partial transformation mutants of RSV. Because fibronectin cables are thought to interact with intracellular stress fibers through focal adhesions (14, 38), we examined rASV 1702- and rASV 157-transformed cells to determine extracellular fibronectin organization in cells with highly

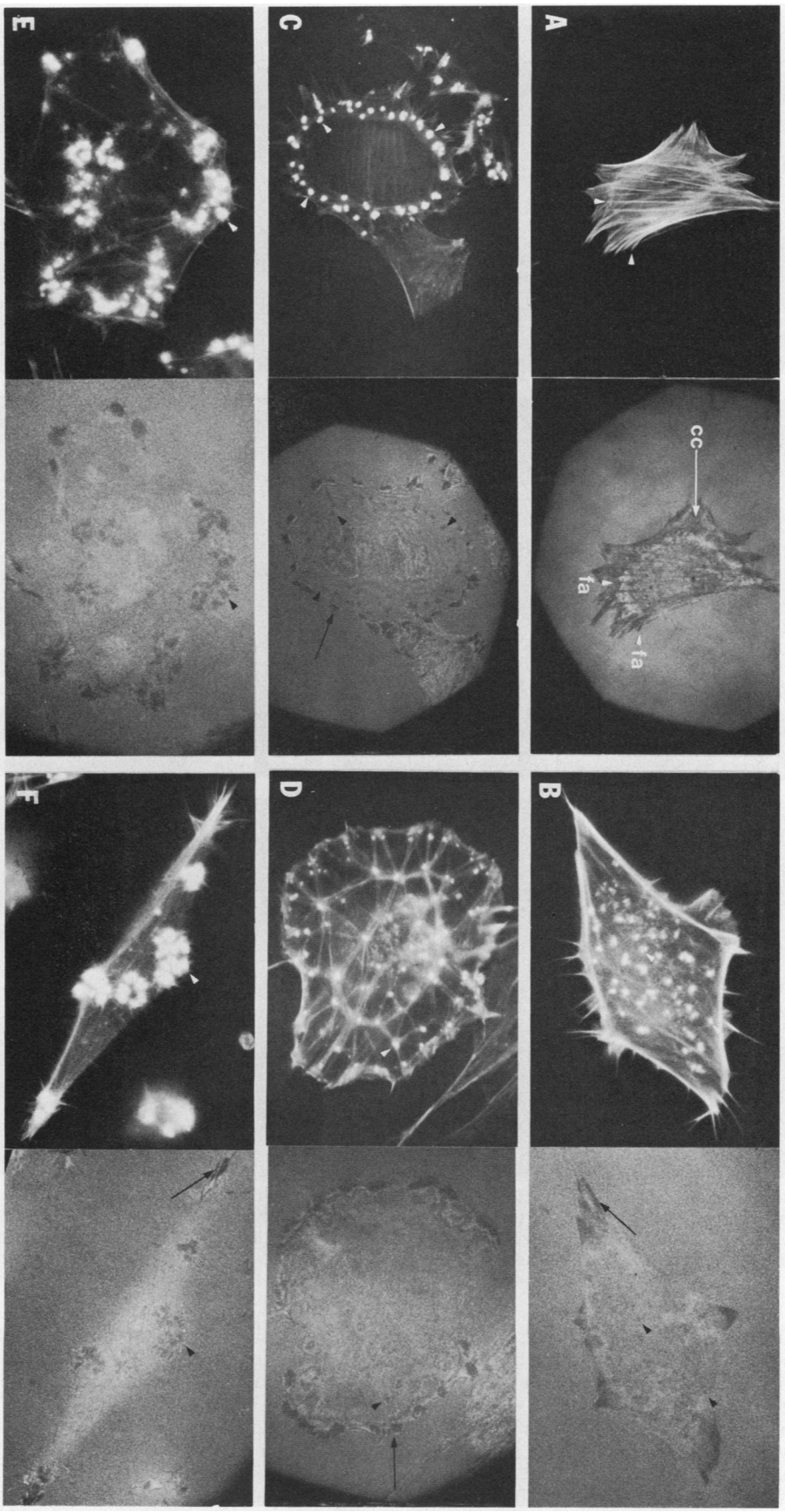

FIG. 5. Microscopic analysis of adhesion plaques in rASV-transformed cells. Paired micrographs of actin fluorescence (left) and the interference reflection image of the same cell (right). The cells are uninfected CEF (A) and CEF tranformed by RSV (B), rASV 3811 (C and D), rASV 157 (E), or rASV 1702 (F). Focal adhesions (fa) and close contacts (cc) are indicated (A). More normal-appearing focal adhesions are indicated by arrows (B through F), whereas punctate adhesions and large adhesion plaque structures are indicated by arrowheads. Focus was set at the ventral cell surface in all micrographs.

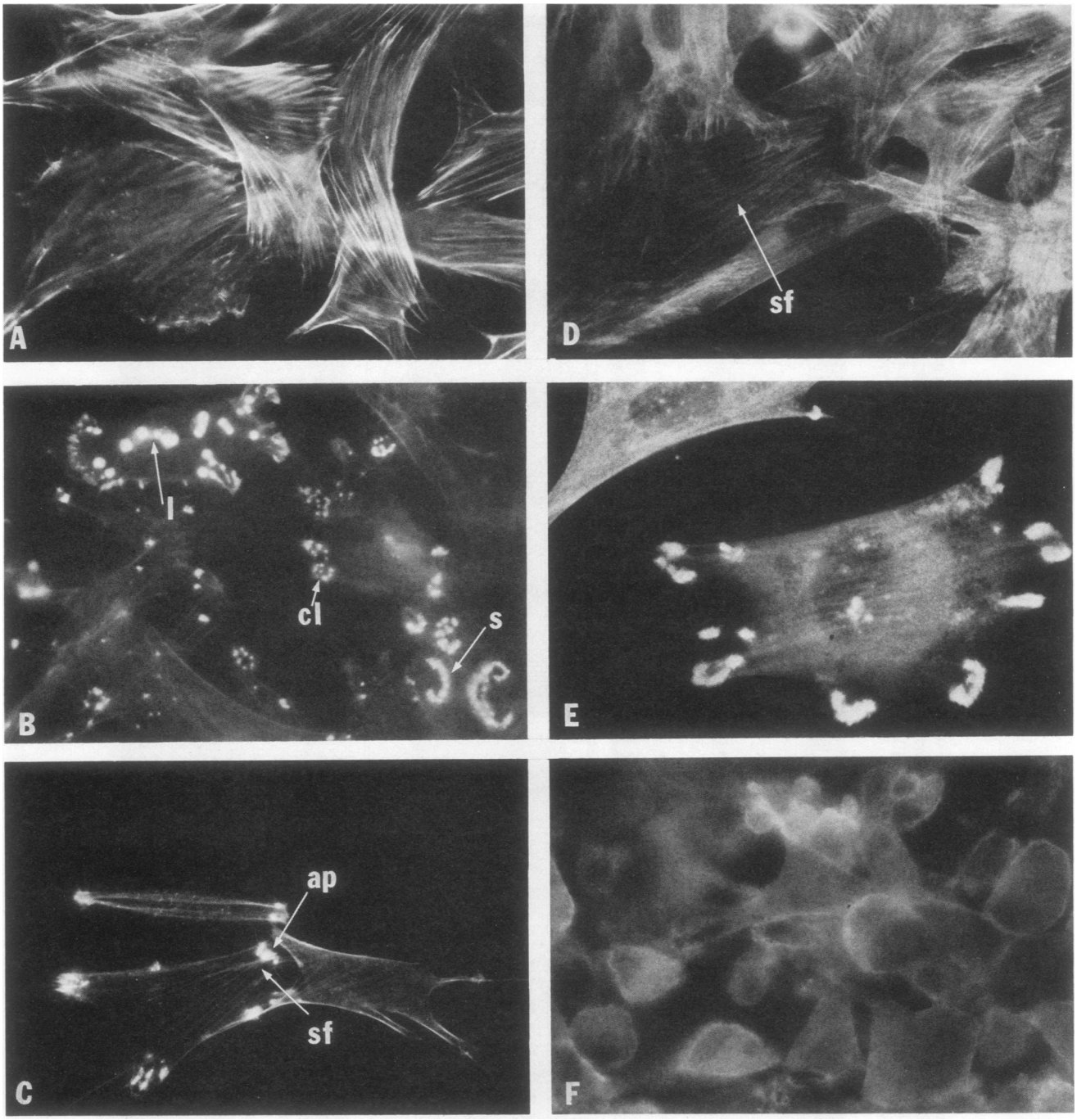

FIG. 6. Organization of actin and filamin in rASV-transformed cells. Cells stained with NBD-phallacidin (A through C) or anti-filamin antibodies by indirect immunofluorescence (D through F). Cells are uninfected CEF (A and D) or CEF transformed by rASV 157 (B and E), rASV 1702 (C), or rASV 3811 (F). The organization of adhesion plaques into linear arrays (l), clusters (c), and scrolls (s) is indicated. Actin stress fibers (sf) are visible in some cells. Focus was set at approximately mid-nuclear level (A, D, and F) or at the ventral cell surface (B, C, and E).

disordered cell-substratum adhesions (Fig. 7). As expected, fibronectin cables are abundant in uninfected CEF cultures (Fig. 7A and B) and are largely absent in CEF transformed by RSV (Fig. 7C and D) and by rASV 3811 (Fig. 7F). However, both rASV 1702- and rASV 157-transformed cultures show retention of extracellular fibronectin cables (Fig. 7G through J).

Interaction with cytoskeleton elements. The degrees of interaction of rASV 1702 pp60^{src} and wild-type RSV pp60^{src} with cytoskeleton matrices were compared under different extraction conditions. Cytoskeleton matrices were prepared by in situ extraction of rASV 1702- or RSV-transformed cells in CSK buffer containing either Mg^{+2} or EDTA and the different KCl concentrations listed in Table 1. rASV 1702 pp60^{src} was easily extracted from the cytoskeleton framework by increasing concentrations of KCl only in the presence of EDTA. Wild-type RSV pp60^{src} is poorly extracted from the cytoskeleton matrix in either Mg^{+2}- or EDTA-containing

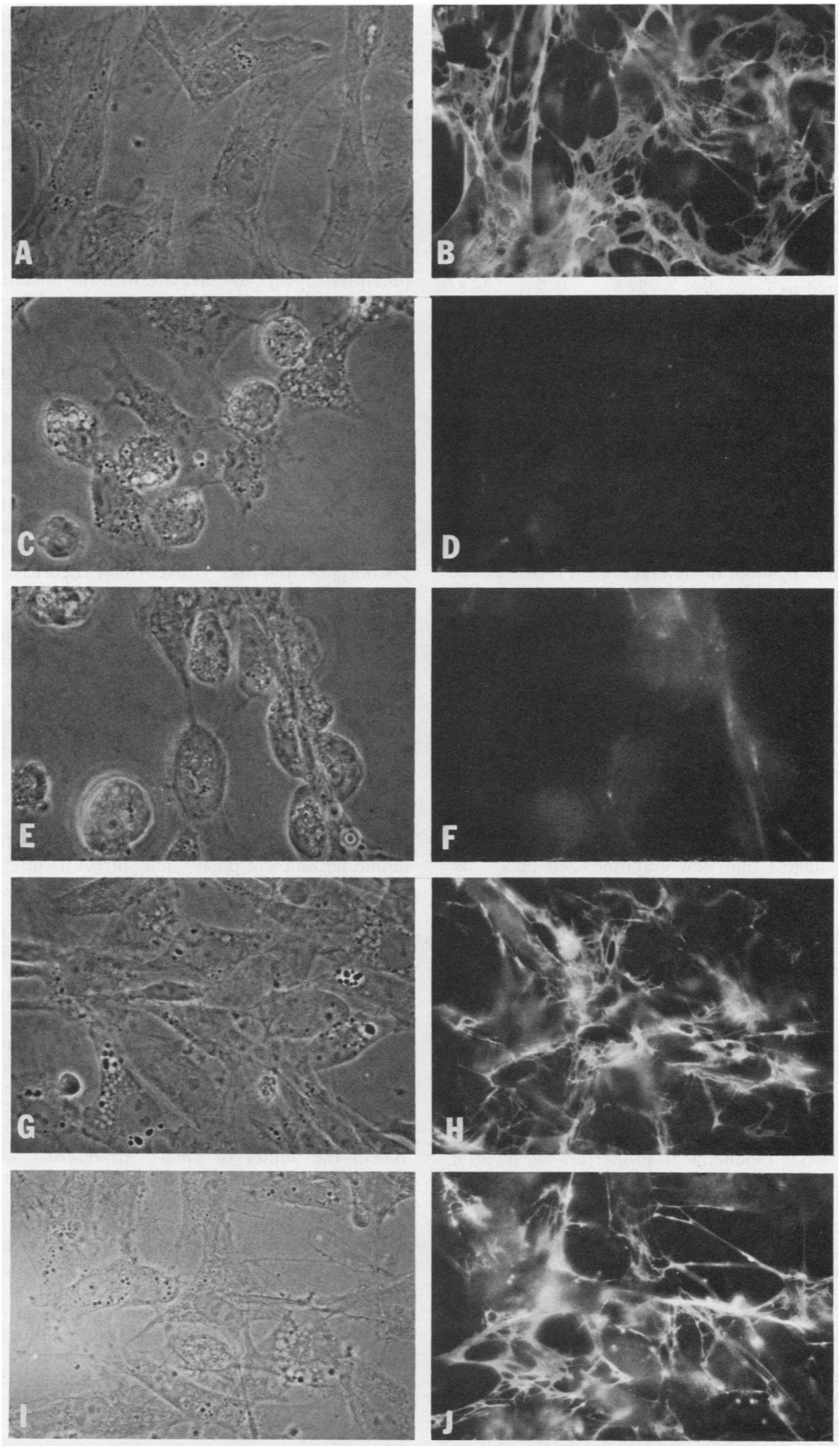

FIG. 7. Expression of extracellular fibronectin. Fibronectin staining by indirect immunofluorescence and phase-contrast micrographs of uninfected CEF (A and B) and CEF transformed by RSV (C and D), rASV 3811 (E and F), rASV 157 (G and H), or rASV 1702 (I and J). Focus was set at approximately mid-nuclear level.

TABLE 1. Binding of pp60^{src} to cytoskeleton matrices prepared from SR-RSV-A[a] or rASV 1702-transformed cells by extraction with CSK buffer containing different ionic compositions

Extraction buffer	% Kinase released into supernatant[b]			
	CSK buffer + Mg^{2+}		CSK buffer + EDTA	
	SR-RSV-A	rASV 1702	SR-RSV-A	rASV 1702
CSK buffer + 10 mM KCl	7.7	2.7	17.3	41.0
CSK buffer + 100 mM KCl	9.3	10.5	19.6	45.8
CSK buffer + 250 mM KCl	9.8	19.5	23.2	52.1
CSK buffer + 500 mM KCl	10.6	27.8	35.7	76.8

[a] SR-RSV-A, Schmidt-Ruppin strain of RSV, subgroup A.
[b] Remaining pp60^{src}-kinase is associated with the cytoskeleton matrix.

CSK buffers (Table 1). The KCl-sensitive binding of rASV 1702 pp60^{src} to the cytoskeleton matrix suggests that it binds to matrix components primarily through divalent cation-mediated electrostatic interactions, though weak hydrophobic interactions also may be involved. In conventional cellular fractionation schemes, the solubilization of rASV 1702 pp60^{src} is not dependent on detergents but is dependent on the ionic composition of the buffer and on the presence of EDTA (data not shown). Since several known cytosolic proteins are readily solubilized in CSK buffer containing 100 mM KCl (6), data shown in Table 1 suggest that rASV 1702 pp60^{src} binds to the cytoskeleton matrix through electrostatic interactions. As adhesion plaques are a component of this cytoskeleton matrix (37; data not shown), these results suggest that the size-variant pp60^{src} proteins might interact with adhesion plaque constitutents principally through ionic interactions.

DISCUSSION

Previous data suggest that newly synthesized pp60^{src} is complexed with two cellular phosphoproteins, pp50 and pp90, and that pp60^{src} may be transported to the plasma membrane in association with these proteins (3, 4, 8). The size-variant rASV-encoded pp60^{src} proteins appear to be similar to wild-type pp60^{src} in this respect since only a small fraction of intracellular pp60^{src} is found in the complexed form and the interaction with this complex occurs transiently, shortly after pp60^{src} biosynthesis. The size-variant pp60^{src} proteins interact with adhesion plaques and intercellular contacts as peripheral membrane proteins (39). These pp60^{src} proteins, however, are not seen in the free cell edge by immunofluorescence microscopy, unlike normal pp60^{src} proteins, which have biochemical properties of integral membrane proteins (37). rASV 1702- and rASV 157-infected cells show partial-transformation phenotypes with respect to fibronectin expression and transformed morphology. Their transformed morphologies may be due to unusual aggregates of adhesion plaques containing pp60^{src}. Focal membrane changes (blebs and microvilli) could be related to focal accumulations of pp60^{src} in the membranes of these cells.

Information about the interaction of pp60^{src} with specific subcellular sites and potential effects on transformation-related properties for CEF transformed by RSV, tsNY68, rASV 3811, rASV 157 and rASV 1702 are listed in Table 2, which also summarizes the data in this study. Studies, using immunofluorescence microscopy and biochemical cellular fractionation to localize pp60^{src} proteins encoded by rASV 1702, rASV 157 and the RSV mutants CU2 and tsNY68, have shown altered interaction of these *src* proteins with the cell (4, 8, 11, 12, 19, 30, 32, 33). The specific nature of these altered subcellular interactions may be especially relevant, since all of these viruses show decreased tumorigenic potential in vivo (1, 16, 18, 19). Three viruses with decreased tumorigenic potential, tsNY68, rASV 1702, and rASV 157, encode pp60^{src} proteins which behave as soluble, cytosolic proteins in cell fractionation studies (Table 2). pp60^{src} appears to interact with plasma membranes as an integral membrane protein in CEF transformed by viruses with normal tumorigenic potential (Table 2). Decreased tumorigenic potential appears to correlate with the absence of pp60^{src} in the free cell edge, i.e., these mutant pp60^{src} proteins do not appear to show widespread or generalized plasma membrane interaction (Table 2). Decreased interaction of pp60^{src} with the free cell edge and decreased tumorigenic potential also seem to correlate with the absence of amino-terminal-bound lipid in these pp60^{src} proteins (Table 2). CEF transformed by rASVs 1702 and 157 (Table 2) and the RSV mutant CU2 (30, 33) show more abundant pp60^{src}-containing adhesion plaques than do CEF transformed by other viruses (Table 2). The interaction of pp60^{src} with adhesion plaques does not correlate with oncogenic potential, since CEF infected with these viruses show only partial-transformation phenotypes and the viruses have decreased tumorigenic potential in vivo (1, 16, 19). Although the presence of pp60^{src} in adhesion plaques was shown previously to correlate with loss of extracellular fibronectin (30), the results of this study indicate that the presence of pp60^{src} in adhesion plaques is not sufficient to induce fibronectin loss.

The interaction of rASV 1702 and 157 pp60^{src} proteins with restricted areas of the plasma membrane poses interesting questions in the analysis of transport and membrane interaction. Whereas pp60^{src} may be transported to the plasma membrane by the pp50-pp90 complex, the details of its subsequent compartmentalization into specific regions of the membrane are unknown. The addition of fatty acid to the amino terminus of pp60^{src} may direct its integration into the plasma membrane. This integrated form appears to correspond to the pp60^{src} in the free cell edge visualized by immunofluorescence (Table 2). rASV 1702 and rASV 157 pp60^{src} proteins do not integrate into the plasma membrane and therefore must interact with specialized regions of the plasma membrane as peripheral proteins. Adhesion plaques are focal accumulations of many different cytoskeleton proteins (13, 30, 40a, 41), and the size-variant pp60^{src} proteins could bind to adhesion plaques through monovalent or divalent ionic bonds with any of these proteins (as suggested by the data in Table 1). The interaction of rASV 1702 and 157 pp60^{src} proteins with regions of cell-to-cell contact may reflect the ability of pp60^{src} to interact with specialized membrane junctions such as pp60^{src} in RSV-transformed rat kidney cells (33). Previous studies in which RSV-transformed rat kidney cells were used have established that only a small fraction of intracellular pp60^{src} is associated with adhesion plaques (37), whereas the remainder is probably found in the plasma membrane as an integral protein (9, 24). Interaction of anti-pp60^{src} antibodies with rASV 1702- or 157-transformed CEF reveals more cytoplasmic fluorescence than that seen in CEF transformed by control viruses (e.g., cf. Fig. 3E and H). Thus, it is possible that only a small fraction of the size-variant pp60^{src} molecules interact with adhesion plaques, whereas the remainder is distributed between other plasma membrane regions and the free cytosol. The designation of the size-variant pp60^{src} proteins as peripheral membrane proteins applies only to those mole-

TABLE 2. Subcellular localization of pp60^{src} proteins encoded by different viruses and some properties of CEF transformed by these viruses[a]

Virus	Tumorigenicity of virus in CEF	Transformed morphology	pp60^{src} interaction with p50-p90 complex	Lipid bound to pp60^{src} (11)[b]	Subcellular localization of pp60^{src} by					Actin stress fibers	Large aggregates of adhesion plaques	Cell surface fibronectin
					Biochemical fractionation	Immunofluorescence microscopy						
						Adhesion plaques	Cell-to-cell contacts	Ruffling membranes	Free cell edge			
SR-RSV-A[c]	Highly tumorigenic (16, 18)	Round, refractile (16)	Free > bound	+	Plasma membrane (21, 26)	− to +	+	+	+	−	−	−
tsNY68 (37°C)	Highly tumorigenic in ovo (28)	Round, refractile (16)	Free > bound (4)	+	Plasma membrane (4, 9, 12)	− to +	+	+	+	−	−	−
tsNY68 (42°C)	Reduced in ovo and in vivo (16, 18, 28)	Flat, normal appearing	Bound > free (5)	Reduced	Soluble cytosol (4, 9, 12)	−	−	−	−	+++	−	+
rASV 1702	Reduced (19)	Spindle form to well spread, dorsal surface blebs and microvilli	Free > bound	−	Soluble cytosol (19)	++	+	+	−	+	+	+
rASV 157	Reduced (19)	Spindle form to well spread, dorsal surface blebs and microvilli	Free > bound	−	Soluble cytosol (19)	++	+	+	−	+	+	+
rASV 3811	Highly tumorigenic (19)	Round to short spindle	Free > bound	+	Plasma membrane (19)	− to +	+	+	+	+	−	−

[a] −, Negative or absent; +, present; ++, increased abundance of pp60^{src} in adhesion plaques; +++, large abundance of actin fibers (similar to uninfected CEF in this respect).

[b] Numbers in parentheses refer to references.

[c] SR-RSV-A, Schmidt-Ruppin strain of RSV, subgroup A.

cules which are membrane associated. An equilibrium between membrane- or adhesion plaque-associated pp60^{src} and cytosolic pp60^{src} may exist which would favor the classification of these pp60^{src} proteins principally as soluble, cytosolic proteins, as suggested by previous cell fractionation results (10, 19).

The pp60^{src} proteins encoded by rASV 1702, rASV 157, and tsNY68 (at 42°C) fractionate predominantly as soluble cytoplasmic proteins in isotonic buffers (4, 8, 12, 19). The results of this study suggest that at least two different classes of soluble pp60^{src} proteins may exist. In tsNY68-infected CEF maintained at 42°C, pp60^{src} is strongly bound to the cytosolic pp50-pp90 complex (3) and fails to interact normally with the plasma membrane (4, 8, 12). The failure of this pp60^{src} to transform CEF at 42°C may be explained by decreased kinase activity, decreased membrane interaction, or a combination of both factors which removes pp60^{src} from interacting with membrane substrates. In contrast, the pp60^{src} proteins encoded by rASVs 1702 and 157 appear to interact transiently with the pp50-pp90 complex and thus may be transported by it. Correspondence between focal membrane changes seen by scanning electron microscopy in these cells and localization of size-variant pp60^{src} proteins in discrete membrane regions suggest that pp60^{src} may need to be in direct association with the plasma membrane to produce characteristic transformation-related changes. Thus, the partial-transformation phenotypes of rASV 1702- and 157-infected CEF might be explained by the failure of these pp60^{src} to interact with critical plasma membrane regions.

rASV 1702-induced tumors contain transformed cells which are morphologically distinguishable from more highly malignant tumor cells in wild-type RSV-induced sarcomas (19). Biochemical properties of rASV 157 and 1702 pp60^{src} proteins which lead to a decreased interaction with membranes of cultured cells would presumably affect the interaction of these molecules with neoplastic cells of adult animals and could lead to the decreased in vivo oncogenic potential of these viruses.

LITERATURE CITED

1. **Anderson, D. D., R. P. Beckmann, E. H. Harms, K. Nakamura, and M. J. Weber.** 1981. Biological properties of "partial" transformation mutants of Rous sarcoma virus and characterization of their pp60^{src} kinase. J. Virol. **37**:445–458.
2. **Barak, L. S., R. R. Yocum, E. A. Nothnagel, and W. W. Webb.** 1980. Fluorescence staining of the cytoskeleton in living cells with 7-nitrobenz-2-oxa-1,3-diazolephallacidin. Proc. Natl. Acad. Sci. U.S.A. **77**:980–984.
3. **Brugge, J. S., E. Erikson, and R. L. Erikson.** 1981. The specific interaction of the Rous sarcoma virus transforming protein, pp60^{src}, with two cellular proteins. Cell **25**:363–372.
4. **Brugge, J. S., W. Yonemoto, and D. Darrow.** 1983. Interaction between the Rous sarcoma virus transforming protein and two cellular phosphoproteins: analysis of the turnover and distribution of this complex. Mol. Cell. Biol. **3**:9–19.
5. **Burr, J. G., G. Dreyfuss, S. Penman, and J. M. Buchanan.** 1980. Association of the *src* gene product of Rous sarcoma virus with cytoskeletal structures of chicken embryo fibroblasts. Proc. Natl. Acad. Sci. U.S.A. **77**:3484–3488.
6. **Burr, J. G., S.-R. Lee, and J. M. Buchanan.** 1981. In situ phosphorylation of proteins associated with the cytoskeleton of chick embryo fibroblasts. Cold Spring Harbor Conf. Cell Proliferation **8**:1217–1232.
7. **Collett, M. S., and R. L. Erikson.** 1978. Protein kinase activity associated with the avian sarcoma virus *src* gene product. Proc. Natl. Acad. Sci. U.S.A. **75**:2021–2024.
8. **Courtneidge, S. A., and J. M. Bishop.** 1982. The transit of pp60^{src} to the plasma membrane. Proc. Natl. Acad. Sci. U.S.A. **79**:7117–7121.
9. **Courtneidge, S. A., A. D. Levinson, and J. M. Bishop.** 1980. The protein encoded by the transforming gene of avian sarcoma virus (pp60^{src}) and a homologous protein in normal cells (pp60^{src}) are associated with the plasma membrane. Proc. Natl. Acad. Sci. U.S.A. **77**:3783–3787.
10. **Feldman, R. A., E. Wang, and H. Hanafusa.** 1983. Cytoplasmic localization of the transforming protein of Fujinami sarcoma virus: salt-sensitive association with subcellular components. J. Virol. **45**:782–791.
11. **Garber, E. A., J. G. Krueger, H. Hanafusa, and A. R. Goldberg.** 1983. Only membrane-associated RSV *src* proteins have amino-terminally bound lipid. Nature (London) **302**:161–163.
12. **Garber, E. A., J. G. Krueger, H. Hanafusa, and A. R. Goldberg.** 1983. Temperature-sensitive membrane association of pp60^{src} in tsNY68-infected cells correlates with increased tyrosine phosphorylation of membrane-associated proteins. Virology **126**:73–86.
13. **Geiger, B.** 1979. A 130K protein from chicken gizzard: its localization at the termini of microfilament bundles in cultured cells. Cell **18**:193–205.
14. **Hynes, R. O., and A. T. Destree.** 1978. Relationships between fibronectin (LETS) protein and actin. Cell **15**:875–886.
15. **Izzard, C. S., and L. R. Lochner.** Cell-to-substrate contacts in living fibroblasts: an interference reflexion study with an evaluation of the technique. J. Cell Sci. **21**:129–159.
16. **Kahn, P., K. Nakamura, S. Shin, R. E. Smith, and M. J. Weber.** 1982. Tumorigenicity of partial transformation mutants of Rous sarcoma virus. J. Virol. **42**:602–611.
17. **Karess, R. E., and H. Hanafusa.** 1981. Viral and cellular *src* genes contribute to the structure of recovered avian sarcoma virus transforming protein. Cell **24**:155–164.
18. **Kawai, S., and H. Hanafusa.** 1971. The effect of temperature on the transformed state of cells infected with a Rous sarcoma virus mutant. Virology **46**:470–479.
19. **Krueger, J. G., E. A. Garber, A. R. Goldberg, and H. Hanafusa.** 1982. Changes in amino-terminal sequences of pp60^{src} lead to decreased membrane association and decreased in vivo tumorigenicity. Cell **28**:889–896.
20. **Krueger, J. G., E. Wang, E. A. Garber, and A. R. Goldberg.** 1980. Differences in intracellular location of pp60^{src} in rat and chicken cells transformed by Rous sarcoma virus. Proc. Natl. Acad. Sci. U.S.A. **77**:4142–4146.
21. **Krueger, J. G., E. Wang, and A. R. Goldberg.** 1980. Evidence that the *src* gene product of Rous sarcoma virus is membrane associated. Virology **101**:25–40.
22. **Krzyzek, R. A., R. L. Mitchell, A. F. Lau, and A. J. Faras.** 1980. Association of pp60^{src} and *src* protein kinase activity with the plasma membrane of nonpermissive and permissive avian sarcoma virus-infected cells. J. Virol. **36**:805–815.
23. **Lee, J. S., H. E. Varmus, and J. M. Bishop.** 1979. Virus-specific messenger RNAs in permissive cells infected by avian sarcoma virus. J. Biol. Chem. **254**:8015–8022.
24. **Levinson, A. D., S. A. Courtneidge, and J. M. Bishop.** 1981. Structural and functional domains of the Rous sarcoma virus transforming protein (pp60^{src}). Proc. Natl. Acad. Sci. U.S.A. **78**:1624–1628.
25. **Levinson, A. D., H. Oppermann, H. E. Varmus, and J. M. Bishop.** 1978. Evidence that the transforming gene of avian sarcoma virus encodes a protein kinase associated with a phosphoprotein. Cell **15**:561–572.
26. **Levinson, A. D., H. Oppermann, H. E. Varmus, and J. M. Bishop.** 1980. The purified product of the transforming gene of avian sarcoma virus phosphorylates tyrosine. J. Biol. Chem. **255**:11973–11980.
27. **Nigg, E. A., B. M. Sefton, T. Hunter, G. Walter, and S. J. Singer.** 1982. Immunofluorescent localization of the transforming protein of Rous sarcoma virus with antibodies against a synthetic *src* peptide. Proc. Natl. Acad. Sci. U.S.A. **79**:5322–5326.
28. **Poirier, F., D. Lawrence, P. Vigier, and P. Jullien.** 1982. A ts T

mutant of Schmidt Ruppin strain of Rous sarcoma virus restricted at 39.5°C for the morphological transformation and the tumorigenicity of chicken embryo fibroblasts. Int. J. Cancer **29**:69–76.

29. **Purchio, A. F., S. Jovanovich, and R. L. Erikson.** 1980. Sites of synthesis of viral proteins in avian sarcoma virus-infected chicken cells. J. Virol. **35**:629–636.
30. **Rohrschneider, L., and M. J. Rosok.** 1983. Transformation parameters and pp60^{src} localization in cells infected with partial transformation mutants of Rous sarcoma virus. Mol. Cell. Biol. **3**:731–746.
31. **Rohrschneider, L. R.** 1979. Immunofluorescence on avian sarcoma virus-transformed cells: localization of the *src* gene product. Cell **16**:11–24.
32. **Rohrschneider, L. R.** 1980. Adhesion plaques of Rous sarcoma virus-transformed cells contain the *src* gene product. Proc. Natl. Acad. Sci. U.S.A. **77**:3514–3518.
33. **Rohrschneider, L. R., M. Rosok, and K. Shriver.** 1982. Mechanism of transformation by Rous sarcoma virus: events within adhesion plaques. Cold Spring Harbor Symp. Quant. Biol. **46**:953–965.
34. **Sefton, B. M., I. S. Towbridge, J. A. Cooper, and E. M. Scolnick.** 1982. The transforming proteins of Rous sarcoma virus, Harvey sarcoma virus, and Abelson virus contain tightly-bound lipid. Cell **31**:465–474.
35. **Shizuta, Y., H. Shizuta, M. Gallo, P. Davies, I. Pastan, and M. S. Lewis.** 1976. Purification and properties of filamin, an actin binding protein from chicken gizzard. J. Biol. Chem. **251**:6562–6567.
36. **Shriver, K., and L. R. Rohrschneider.** 1981. Organization of pp60^{src} and selected cytoskeletal proteins within adhesion plaques and junctions of Rous sarcoma virus-transformed rat cells. J. Cell Biol. **89**:525–535.
37. **Shriver, K., and L. R. Rohrschneider.** 1981. Spatial and enzymatic interaction of pp60^{src} with cytoskeletal proteins in isolated adhesion plaques and junctions from RSV-transformed NRK cells. Cold Spring Harbor Conf. Cell Proliferation **8**:1247–1262.
38. **Singer, I., and P. R. Paradiso.** 1981. A transmembrane relationship between fibronectin and vinculin (130 kd protein): serum modulation in normal and transformed hamster fibroblasts. Cell **24**:481–492.
39. **Singer, S. J.** 1974. The molecular organization of membranes. Annu. Rev. Biochem. **43**:805–833.
40. **Wang, E., and A. R. Goldberg.** 1976. Changes in microfilament organization and surface topography upon transformation of chick embryo fibroblasts with Rous sarcoma virus. Proc. Natl. Acad. Sci. U.S.A. **73**:4065–4069.

40a. **Wang, E., H. L. Yin, J. G. Krueger, L. A. Caliguiri, and I. Tamm.** 1983. Unphosphorylated gelsolin is localized in regions of cell-substratum contact or attachment in Rous sarcoma virus-transformed rat cells. J. Cell Biol. **98**:761–771.

41. **Wehland, J., M. Osborn, and K. Weber.** 1979. Cell-to-substratum contacts in living cells: a direct correlation between interference-reflection and indirect-immunofluorescence microscopy using antibodies against actin and α-actinin. J. Cell Sci. **37**:257–273.
42. **Willingham, M. C., G. Jay, and I. Pastan.** 1979. Localization of ASV *src* gene product to the plasma membrane of transformed cells by electron microscopic immunocytochemistry. Cell **18**:125–134.